

STRANGE QUARK STARS IN BINARIES: FORMATION RATES, MERGERS AND EXPLOSIVE PHENOMENA

G. WIKTOROWICZ¹, A. DRAGO², G. PAGLIARA², S.B. POPOV³

¹ Astronomical Observatory, University of Warsaw, Al. Ujazdowskie 4, 00-478 Warsaw, Poland (*gwiktoro@astroww.edu.pl*)

² Dip. di Fisica e Scienze della Terra dell'Università di Ferrara and INFN Sez. di Ferrara, Via Saragat 1, I-44100 Ferrara, Italy

³Sternberg Astronomical Institute, Lomonosov Moscow State University, Universitetsky prospekt 13, 119234, Moscow, Russia

Draft version September 25, 2017

ABSTRACT

Recently, the possible co-existence of a first family composed of "normal" neutron stars with a second family of strange quark stars has been proposed as a solution of problems related to the maximum mass and to the minimal radius of these compact stellar objects. In this paper we study the mass distribution of compact objects formed in binary systems and the relative fractions of quark and neutron stars in different subpopulations. We incorporate the strange quark star formation model provided by the two-families scenario and we perform a large-scale population synthesis study in order to obtain the population characteristics. According to our results, the main channel for strange quark star formation in binary systems is accretion from a secondary companion on a neutron star. Therefore, a rather large number of strange quark stars form by accretion in low-mass X-ray binaries and this opens the possibility of having explosive GRB-like phenomena not related to supernovae and not due to the merger of two neutron stars. The number of double strange quark star's systems is rather small with only a tiny fraction which merge within a Hubble time. This drastically limits the flux of strangelets produced by the merger, which turns out to be compatible with all limits stemming from Earth and Lunar experiments. Moreover, this value of the flux rules out at least one relevant channel for the transformation of all neutron stars into strange quark stars by strangelets' absorption.

Subject headings: Stars: neutron stars, strange quark stars, X-ray: binaries, Methods: statistical

1. INTRODUCTION

The discovery, in 2010, of a pulsar with a mass of about two solar masses (Demorest et al. 2010) has stimulated many theoretical studies, in the nuclear astrophysics community, concerning its possible composition and the properties of the equation of state of dense matter. It is clear indeed that the center of this stellar object could be the site of the most dense form of nuclear matter we are aware of: depending on the adopted model for the equation of state, the central density of this star could be larger than about 3 times the nuclear saturation density. There are many different ideas on the composition of matter at such a high density: for instance, hyperons (Chatterjee & Vidaña 2016) or delta resonances (Drago et al. 2014b) could form, or a phase transition to quark matter could occur (Alford et al. 2015). The need to fulfill the two solar mass limit provides tight microphysical constraints on those scenarios.

It is clear that precise mass measurements represent a powerful and reliable tool to investigate the properties of dense matter. Future observations (e.g. by the FAST (Nan et al. 2011) and SKA radio telescopes (Carilli & Rawlings 2004)) could possibly prove the existence of even larger masses. However, some information could be obtained also by considering the (much more uncertain) measurements of the radii. Unfortunately, up to now, only in a few cases mass and radius of a same compact star have been estimated from x-ray analysis and moreover with large systematic uncertainties (Özel & Freire 2016; Miller & Lamb 2016). Although still under debate, there are a few indications of the possible existence of stellar objects with radii smaller than about 11 km

(Guillot & Rutledge 2014; Özel et al. 2016), thus very compact. Very small radii for stars having masses of about 1.4 – 1.5 M_{\odot} are obtained only if the equation of state of dense matter is very soft at densities of about 2 – 3 times nuclear matter saturation density. On the other hand, so soft equations of state lead to maximum masses significantly smaller than 2 M_{\odot} , because to reach very large masses would imply an extreme stiffening of the equation of state at larger densities, saturating the limit of causality, a situation that is not very realistic (Alford et al. 2015). If future observations with new facilities, such as the NICER experiment on-board ISS (Gendreau et al. 2012), will confirm the existence of very compact stars, then one has to explain how the equation of state of dense matter could be at the same time very soft (to explain the very compact configurations) and very stiff (to explain the very massive configurations).

In Drago et al. (2014a); Drago et al. (2016); Drago & Pagliara (2016), a possible solution to this puzzle has been proposed. It is based on the existence of two families of compact stars: neutron Stars (NSs indicating both stars made of nucleons and stars containing hyperons) which are compact and light, and strange quark stars (QSs) (Alcock et al. 1986; Haensel et al. 1986) which are large and massive (a 2 M_{\odot} star would be a QS for instance). In this scenario, strange quark matter composed of three flavors: up, down, and strange, is the true ground state and hadronic matter is instead metastable. A NS could therefore convert into a QS once a significant fraction of strangeness is formed in its interior through the appearance of hyperons and the conversion time turns out to be of the order of ten seconds (Drago et al. 2007; Herzog & Röpke 2011; Niebergal et al. 2010; Pagliara

et al. 2013; Drago & Pagliara 2015). The critical density for such a transition is thus close to the threshold of hyperons’ formation¹. The exact value of the density at which hyperons start forming depends on the microphysics of the equation of state and it determines the maximum mass and the minimum radius of NSs (in this paper we do not consider rotating configurations). The smaller the minimum radius the smaller the maximum mass. Since we are interested in radii smaller than about 11 km, then the limiting gravitational mass of a NS is $M_{\text{max}}^H \sim 1.5\text{--}1.6 M_{\odot}$. As shown in Fig.1, the unstable hadronic star forms a QS having the same baryonic, but a smaller gravitational mass. The “mass defect” is $\Delta M \sim 0.1\text{--}0.15 M_{\odot}$. One can infer therefore that within the two-families scenario the mass distribution would be qualitatively different with respect to the one of the standard one-family scenario: we expect, in particular, an enhancement in the number of stars with masses in the range $(M_{\text{max}}^H - \Delta M) \leq M \leq M_{\text{max}}^H$ (co-existence range), compensated by a depopulation of the the region of masses larger than M_{max}^H , a feature that could be possibly tested by means of future observations of the FAST and SKA radio telescopes.

We will focus here on binary systems with QSs, as they allow for the dynamical mass measurement of a compact object. There exist three general ways a QS can form during the evolution of a binary system²:

1. The binary components may not interact during their evolution (single-star-like evolution). It requires a star having an initial mass $M_{\text{ZAMS}} \approx 18\text{--}22 M_{\odot}$;
2. The star may become a NS with a mass $M_{\text{NS}} < M_{\text{max}}^H$, and then accrete material from the companion to become a QS afterwards (e.g., Cheng & Dai 1996; Dai & Lu 1998; Zhu et al. 2013; Jiang et al. 2015). In this channel the initial mass range is much wider ($M_{\text{ZAMS}} \approx 6\text{--}17.5 M_{\odot}$) and more populated than in the previous case;
3. The third possibility involves mass-loss by a massive progenitor due to binary interactions: mass transfer (MT) or common envelope (CE). As a result, the mass of the post-supernova (SN) compact object will be lower than in the single-star evolution (for the same initial stellar mass). Instead of forming a black hole (BH), the star finishes its evolution producing a QS. The pre-SN mass-loss is necessary for initial stellar masses $M_{\text{ZAMS}} \gtrsim 22 M_{\odot}$. It may be so prominent that the star will initially form a NS and transform into a QS only after a mass-accretion phase (see the second channel above).

There are two particularly relevant results to be obtained: an estimate of the number of QS-QS systems and of the number of low-mass X-ray binaries (LMXBs) containing a QS. The first number determines the number of

¹ The critical fraction of hyperons needed to trigger the conversion can be estimated by requiring that the strange quark matter phase with the same strangeness fraction is energetically favored Iida & Sato (1998); Bombaci et al. (2004)

² A further possibility is to form a strange quark star through the merger of two neutron stars, but this scenario will not be analyzed in this paper.

double QS (DQS) mergers (note that by DQS we denote only systems consisting of two QSs), which in turn is related to the flux of strangelets ejected at the moment of the merger. Those strangelets can potentially trigger the conversion of all NSs into QSs (Madsen 1988, 2005) therefore invalidating the two-families scenario. We will address this problem in Sec 3.3. The number of LMXBs containing a QS is potentially related to the number of (long) γ -ray bursts generated by the exothermic NS to QS transition in a rapidly rotating neutron star (Drago & Pagliara 2015). This scenario could correspond to GRB060614 in which a long γ -ray burst (GRB) was not accompanied by a supernova (Fynbo et al. 2006; Della Valle et al. 2006; Gal-Yam et al. 2006).

2. MODELING

We performed a simulation of 2 million binaries using the StarTrack population synthesis code (Belczynski et al. 2002b, 2008) with some further amendments (see Wiktorowicz et al. 2015, and references therein). These large-scale simulation were obtained with a use of the Universe@Home project³. Population synthesis method was previously widely used to similar tasks (e.g. Popov & Prokhorov 2007)

We simulated a grid of six models with three different metallicities: Z_{\odot} (solar metallicity; $Z_{\odot} = 0.02$; Villante et al. 2014), $Z_{\odot}/10$, and $Z_{\odot}/100$; and two values of M_{max}^H parameter: 1.5 and 1.6 M_{\odot} .

For initial stellar mass distribution we used the Kroupa et al. (1993) broken power-law with $\alpha = -2.3$ for stars heavier than 1 M_{\odot} . For a primary we chose a mass range of 6–150 M_{\odot} to involve all possible progenitors of compact objects. For secondaries we studied a wider range of 0.08–150 M_{\odot} keeping the mass ratio distribution uniform ($P(q) = \text{const}$). Initial binary separations had the log-uniform distribution — so-called Öpik law, — ($P(a) \sim 1/a$; Abt 1983), whereas, the eccentricity distribution was assumed to be thermal ($P(e) = 2e$; Duquennoy & Mayor 1991). We assumed that the natal kick acts only during NS formation (single-mode Maxwellian distribution with $\sigma = 265 \text{ km s}^{-1}$).

2.1. Strange quark star formation

In this study every NS with a mass $M_{\text{NS}} \geq M_{\text{max}}^H$ transforms into a QS. The transition is so rapid that it occurs within a single time step of our simulation (Drago & Pagliara 2015). In our results the maximum post-SN NS mass was 1.924 M_{\odot} , which transforms into a 1.779 M_{\odot} QS. (initially more massive objects form BH). However, mass accretion may make QSs even heavier.

To calculate the post-transition QS mass we implement the conservation of the baryonic mass (Bombaci & Datta 2000) while the gravitational mass changes due to the different binding energies of NSs and of QSs (see Fig. 1).

The radius in the model we use is larger for a QS. It is irrelevant for the present study, but quite crucial in the interpretation of the two-families model. The maximum gravitational mass of a QS is not well-determined. In our calculations we assume the value of 2.5 M_{\odot} (thus well above all known massive NSs: Demorest et al. (2010); Antoniadis et al. (2013)). A possible way of determining

³ <http://universeathome.pl>

M_{\max}^Q is through the analyses of the extended emission of short GRBs (Lasky et al. 2014; Lu et al. 2015; Li et al. 2016). In particular in Lasky et al. (2014) the expected mass distribution for the post-merger remnant is $M = 2.46^{+0.13}_{-0.15} M_{\odot}$. Although this limit includes also supramassive stars, it represents a hint of the existence of stars with masses significantly larger than $2M_{\odot}$.

A very crucial feature of our scheme is that the radius of the compact star increases during the conversion. This is compatible with a combustion mode which is not driven by pressure but by diffusion (Olinto 1987) and is strongly accelerated by Rayleigh-Taylor hydrodynamical instabilities, as discussed in Horvath & Benvenuto (1988); Drago et al. (2007); Herzog & Röpke (2011); Pagliara et al. (2013); Drago & Pagliara (2015); Furu-sawa et al. (2016). However, these instabilities halt below a certain critical density and the conversion of the most external layer is much slower, see also the recent simulations of Ouyed et al. (2017).

The present analysis does not contain two potentially relevant phenomena which can take place in association with quark deconfinement. First, the impact of quarks deconfinement on the SN explosion is not discussed in this paper: we only assume that if the compact star produced by the SN has a mass larger than M_{\max}^H then it immediately becomes a QS. On the other hand, quark deconfinement could help heavy progenitors to explode (Drago et al. 2008; Drago & Pagliara 2016). This mechanism could in principle produce compact stars with higher masses. Second, we do not take into account the relation between mass accretion and angular momentum accretion. More explicitly, in the present paper rotation is not considered.

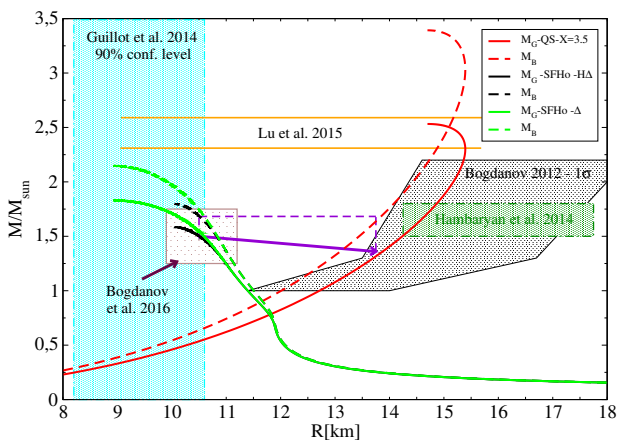


FIG. 1.— The mass-radius relations for hadronic stars and strange quark stars. The dashed lines represent the baryonic masses, whereas the solid lines represent the gravitational masses. A typical transition for a NS reaching M_{\max}^H is shown with violet color. The solid arrow starts at M_{\max}^H and ends at $M_{\max}^H - \Delta M$. Although the baryonic masses before and after the transition are equal (dashed horizontal violet line), the QS gravitational mass is smaller ($M_{\max}^H - \Delta M = 1.36M_{\odot}$) than the NS gravitational mass ($M_{\max}^H = 1.5M_{\odot}$). The maximum mass of the QS branch M_{\max}^Q is significantly larger than M_{\max}^H . The brown box is a rough approximation of the limits indicated in Bogdanov et al. (2016).

TABLE 1
NUMBER OF QS/NS IN BINARIES

Metallicity	#QS ^a	#NS ^a	f_{QS} ^b	#NS(noQS) ^c	f_{cr} ^d
ALL					
Z_{\odot}	9.0×10^4	7.2×10^6	0.01	7.3×10^6	1.10
$Z_{\odot}/10$	2.7×10^5	7.4×10^6	0.04	7.7×10^6	1.37
$Z_{\odot}/100$	1.5×10^5	1.0×10^7	0.01	1.0×10^7	1.57
LMXB					
Z_{\odot}	1.6×10^4	6.1×10^4	0.26	7.7×10^4	1.61
$Z_{\odot}/10$	1.2×10^4	1.5×10^5	0.08	1.6×10^5	1.22
$Z_{\odot}/100$	7.0×10^3	2.1×10^4	0.25	2.9×10^4	1.31
DQS/DNS					
Z_{\odot}	–	6.4×10^5	–	6.6×10^5	0.88
$Z_{\odot}/10$	4.2×10^3	5.2×10^5	0.08	5.2×10^5	1.22
$Z_{\odot}/100$	–	7.6×10^5	–	7.6×10^5	0.86

NOTE. — QS and NS quantities per MWEG at present time for $M_{\max}^H = 1.5 M_{\odot}$. ALL – all binaries; LMXB – mass-transferring binaries; DQS/DNS – double QS/NS.

^a Number of QS (#QS) and NS (#NS)

^b fraction of QSs; defined as $f_{\text{QS}} := \#QS / (\#QS + \#NS)$

^c number of NSs in the model without QSs (noQS)

^d change in a number of compact objects (QSs and NSs) in $1.36 - 1.5 M_{\odot}$ mass range; $f_{\text{cr}} := (\#QS' + \#NS') / \#NS'(\text{noQS})$ (mass range marked with ')

3. RESULTS

The results are scaled to be comparable with the Milky-Way equivalent galaxy (MWEG), which we assumed to have a total stellar mass of $M_{\text{MWEG}} = 6.0 \times 10^{10} M_{\odot}$ (e.g., Licquia & Newman 2015) and continuous star formation. We chose $M_{\max}^H = 1.5 M_{\odot}$, as our standard model and quantitative results refer to this model unless differently stated. In Sec. 3.4 the effects of changing the value of the maximum mass of hadronic stars to $M_{\max}^H = 1.6 M_{\odot}$ are analyzed. We show that the results and conclusions are qualitatively similar for both models.

The ratio of the number of QSs to NSs is between 0.01–0.04 depending on metallicity (Tab. 1), but for mass-transferring binaries (in the case of LMXBs) it is higher: 0.08–0.26. This corresponds to $0.9 - 2.7 \times 10^5$ QSs in a MWEG. Most of them are existing in wide and therefore non-interacting binaries, or are in pairs with low-luminosity companions, which in most cases (78–95%) are white dwarfs (WD).

Fig. 2 demonstrates the effect of deconfinement on the compact stars' (QS/NS) mass distribution in comparison to the model without deconfinement (noQS). Notice specifically that in the range $1.1 - 1.5 M_{\odot}$, where most of the NSs reside, the difference is minimal. In particular, the deconfinement does not affect the peak in the distribution at $\sim 1.3 M_{\odot}$.

3.1. Formation of QSs

Mostly, a QS forms from a primary (i.e. the more massive component in the binary on ZAMS). In $\sim 72 - 96\%$ of cases a QS forms as a consequence of MT onto a NS (route $\mathcal{R}_{A,\text{acc}}$). Only the remaining $\sim 2 - 10\%$ of QSs form directly after a SN explosion ($\mathcal{R}_{A,\text{dir}}$). Rarely ($\leq 20\%$), a QS may form from a secondary, if it is initially massive ($\mathcal{R}_{B,\text{dir}}$; $\sim 18 - 30 M_{\odot}$). Most of these QSs do not interact with their companions, but in about 3–18%

TABLE 2
FORMATION OF STRANGE QUARK STARS IN BINARIES

Typical evolutionary route ^a		#QS per MWEG		
		Z_{\odot}	$Z_{\odot}/10$	$Z_{\odot}/100$
$\mathcal{R}_{A,acc}$	CE1(6-1;12-1) MT2(12-3) AICNS1 MT2(13-3) AICQS1	8.6×10^4	2.1×10^5	1.2×10^5
$\mathcal{R}_{A,dir}$	CE1(4/5-1;7/8-1) SNQS1	4.0×10^3	2.6×10^4	3.2×10^3
$\mathcal{R}_{B,dir}$	MT1(2-1) SN1 CE2(14-4;14-7) SNQS2	6.5×10^2	2.8×10^4	2.7×10^4
\mathcal{R}_{LMXB}	CE1(6-1;12-1) CE2(12-3;12-7) MT2(12-7) AICNS1 MT2(13-7/8) AICQS1 MT2(13-11/17)	1.6×10^4	1.2×10^4	7.0×10^3
\mathcal{R}_{DQS}	MT1(4-4) CE2(7-4;7-7) SNQS1 SNQS2	–	4.2×10^3	–

NOTE. — QS formation channels: $\mathcal{R}_{A,acc}$ – QS forms from a NS due to mass-accretion; $\mathcal{R}_{A,dir}$ – QS form directly after SN; $\mathcal{R}_{B,dir}$ – QS forms from a secondary (less-massive star on ZAMS); \mathcal{R}_{LMXB} – QS in LMXB (mass-transfer present); \mathcal{R}_{DQS} – double QS.

^a Only most important evolutionary phases are present: MT1/2 – mass transfer from the primary/secondary; CE1/2 – common envelope (primary/secondary is a donor); AICNS1 – accretion induced collapse of a WD into a NS; AICQS1 – accretion induced collapse of a NS into a QS; SNQS1/2 – direct formation of a QS after supernova of the primary/secondary. Stellar types: 1 – main sequence; 2 – Hertzsprung Gap; 3 – red giant; 4 – core He-burning; 5/6 – early/thermal pulsing asymptotic giant branch; 7 – He star; 8 – evolved He star; 11 – Carbon-Oxygen White Dwarf; 12 – Oxygen-Neon white dwarf; 13 – neutron star; 14 – black hole; 17 – Hybrid white dwarf.

TABLE 3
TYPICAL PARAMETERS FOR FORMATION CHANNELS

Parameter ^a	$\mathcal{R}_{A,acc}$	$\mathcal{R}_{A,dir}$	$\mathcal{R}_{B,dir}$	\mathcal{R}_{LMXB}	\mathcal{R}_{DQS} ^b
$M_a [M_{\odot}]$	1.4–1.8	1.4–1.7	1.4–1.8	1.4–1.6	1.4–1.6
$M_b [M_{\odot}]$	0.3–0.4	$\lesssim 0.7$	7.8–30	$\lesssim 0.2$	~ 1.7
$a [R_{\odot}]$	$\lesssim 170$	$\gtrsim 4600$	$\lesssim 540$	$\gtrsim 1.9$	7.5–24
$t_{age} [Myr]$	$\gtrsim 8000$	4.2–6000	5.1–6500	900–2600	140–6600
$M_{ZAMS,a} [M_{\odot}]$	6.1–7.8	16–28	18–30	6.0–12	21–24
$M_{ZAMS,b} [M_{\odot}]$	1.0–1.5	2.0–4.1	41–77	0.7–4.7	20–23
$a_{ZAMS} [R_{\odot}]$	560–2200	2900–4500	560–8000	700–2700	570–1200

NOTE. — The table presents the typical values of strange quark star and companion masses and their separation for the present time and ZAMS. In case of the present time, the age of the system is also provided. Scenarios' designations are explained in Tab. 2 and in Sec. 3.1.

^a M_a – QS mass; M_b – companion mass; a – separation; t_{age} – age of the system (time since ZAMS)

^b Both components are QSs

of cases a LMXB can form (\mathcal{R}_{LMXB} ; Sec. 3.2). If the metallicity is moderate ($Z = Z_{\odot}/10$) double QSs form as a result of binary evolution (\mathcal{R}_{DQS} ; Sec. 3.3). Tables 2 and 3 summarize the most typical evolutionary routes for all scenarios. Although models for different metallicities share the same trends, there are differences in the total number and relative abundances of QSs formed via different channels.

$\mathcal{R}_{A,acc}$; *QS forms through accretion onto a NS*— This is the most typical formation scenario of QSs in binaries. In a typical case, a primary is about $7.2 M_{\odot}$ and a secondary is $1.2 M_{\odot}$. The primary evolves faster and fills the Roche lobe (RL) while being on the asymptotic giant branch after 53 Myr. The MT is usually unstable due to large mass ratio and a common envelope (CE) occurs. If the binary survives this phase, the primary is ripped off its hydrogen envelope and becomes an Oxygen-Neon WD with a mass of about $1.3 M_{\odot}$. Afterwards, the secondary evolves, becomes a red giant (RG) and fills its RL. A MT from the secondary increases the mass of the WD up to $1.38 M_{\odot}$. Then the primary collapses and becomes a $1.26 M_{\odot}$ NS. Afterwards, the secondary re-fills the RL and commences a MT again. The system becomes a LMXB. The NS mass may rise up to $1.5 M_{\odot}$ due to accretion and the deconfinement transforms it into a QS with a mass of $1.36 M_{\odot}$ (Fig. 4, upper plot). The MT may proceed further, what will allow the QS to reach a higher mass (typically

up to $1.8 M_{\odot}$). The evolution leads to the formation of a QS-WD system, which is usually too wide to interact anymore.

As already remarked before, here we do not consider the effect of rotation on the structure of compact stars. As discussed in Bejger et al. (2011), the central density during mass accretion could increase marginally due to the simultaneous increase of the angular momentum. Therefore the conversion of the NS could occur either during the mass accretion stage or after the end of mass accretion during the spin down.

$\mathcal{R}_{A,dir}$; *Direct collapse to a QS after a SN explosion*— The initial binary is more massive than in $\mathcal{R}_{A,acc}$ scenario. The primary's initial mass is about $16–28 M_{\odot}$ and the secondary's mass is $\sim 2.0–4.1 M_{\odot}$. When the primary fills its RL, the MT is unstable, so the CE phase commences. The secondary is massive enough to eject the envelope and the system survives with a much shorter orbit (due to orbital angular momentum loss). Additionally, the outer envelope of the primary is ripped off. The SN explosion, which occurs shortly after, may significantly change the separation. Usually no further interaction is observed and the secondary evolves unaffected and forms a WD after ~ 1 Gyr.

The main factor that affects the ratio of QS formation in two above routes is the mass of the components on

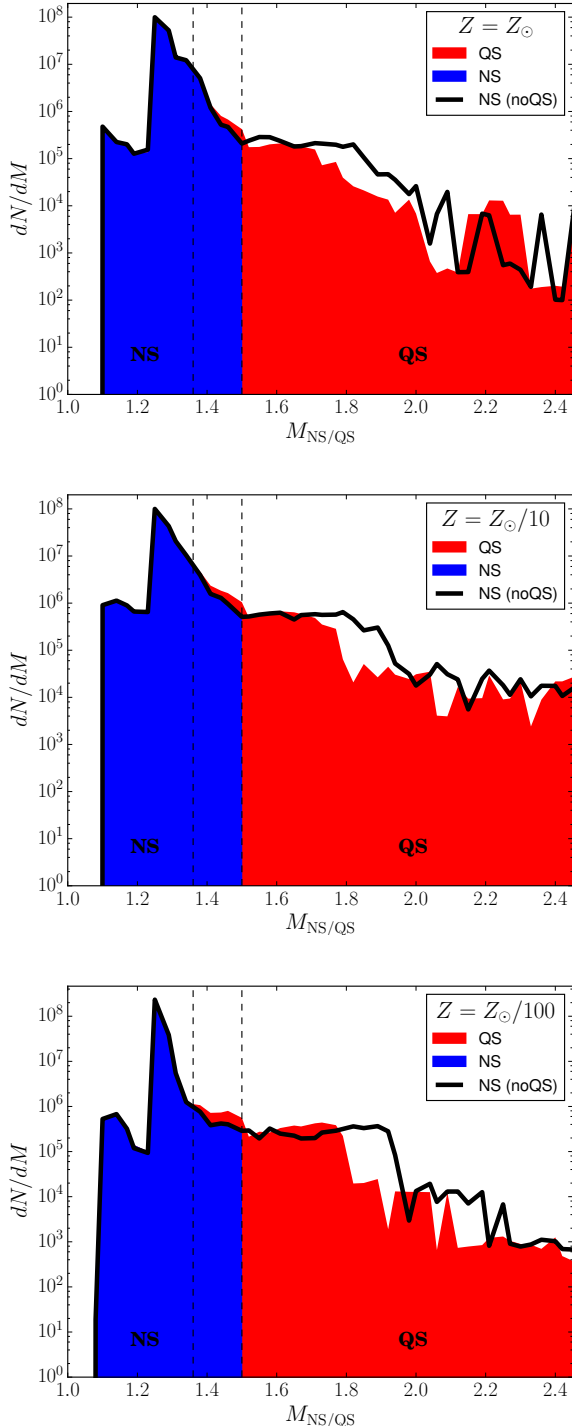


FIG. 2.— The distribution of masses for NS (blue) and QS (red) for metallicity $Z = Z_{\odot}$ (upper plot), $Z = Z_{\odot}/10$ (middle plot), and $Z = Z_{\odot}/100$ (lower plot). The black line marks the distribution of NSs in model without QSs (noQS). Features seen in the QS mass distribution are related to post-QS-formation evolution and are not a subject of this study.

ZAMS. Progenitors of QSs in $\mathcal{R}_{A,acc}$ are lighter, therefore, are more abundant (approximately twice) in the initial populations, then in the case of $\mathcal{R}_{A,dir}$. Additionally, in the case of a heavy primary ($\mathcal{R}_{A,dir}$) it is hard for the secondary to eject the massive envelope of a primary

during CE phase, which frequently leads to a merger. On the other hand, without a CE a system is still wide during a SN. Consequently, it is frequently disrupted (in $\sim 98\%$ of cases).

The companions in $\mathcal{R}_{A,acc}$ are usually low-mass WDs, in agreement with the results by Popov & Prokhorov (2005), who found that many of the most massive uncollapsed compact objects might be observed at the stage of accretion which lasts for a long time. After accretion is over the QS is spun-up and can be observed as a millisecond radio pulsar.

$\mathcal{R}_{B,dir}$; *QSs from secondaries*— QSs formed from secondaries, i.e. less massive binary components on ZAMS, constitute only a small fraction ($\leq 20\%$) of the QS population and the fraction is in general larger for lower metallicity (Tabs. 2 and 4). Primaries in these systems evolve faster than the QS progenitors and usually become BHs.

On ZAMS the binary consist of a $\sim 41-77 M_{\odot}$ primary and $\sim 18-30 M_{\odot}$ secondary. The separation is short enough that when the primary enters the Hertzsprung-Gap (HG) phase its RL is filled. The MT is non-conservative. A BH forms directly after a SN explosion with small mass loss (typically, BHs obtain low natal kicks). Its mass is between $7.8-30 M_{\odot}$. A few Myr later, the secondary fills its RL while being on the core helium burning. The CE occurs in which the separation is shortened and the star loses its outer hydrogen envelope. The second SN results in a direct formation of a QS and the binary becomes a double compact object (BH-QS).

3.2. Low-mass X-ray binaries

We performed a separate analysis for accreting QS. We considered all mass-transferring binaries with NS/QS accretors. Initial donor masses are in general below $3 M_{\odot}$, as heavier companions usually provide dynamically unstable MT. Properties of X-ray emission from accreting NSs or QSs are similar (Alcock et al. 1986), therefore, accreting QSs constitute a subgroup of LMXBs.

Although most of the QSs form through accretion from a RG companion ($\mathcal{R}_{A,acc}$), the MT phase is relatively short and the resulting QS-WD binary is too wide to commence Roche lobe overflow. Consequently, the evolutionary route leading to the formation of a LMXB with a QS is different. We found that a typical companion is a WD with a very small mass ($\lesssim 0.2 M_{\odot}$). It is a direct consequence of a prolonged mass transfer onto the primary. The separation which allows for a Roche lobe overflow is small ($\lesssim 1.9 R_{\odot}$) and the period is very short ($P \lesssim 6$ h).

\mathcal{R}_{LMXB} ; *Accretion onto a QS*— The initial evolution towards the formation of a LMXB with a QS is in general similar to $\mathcal{R}_{A,acc}$, however, secondaries are on the average more massive on ZAMS. As a result, the heavier RG companion after the first CE provides unstable MT, which results in a second CE phase (this time the secondary is a donor). The orbit shrinks and the secondary loses much of its mass ($\sim 80\%$). The resulting helium star ($M_b \approx 0.7 M_{\odot}$) re-fills the RL and transfers mass onto a heavy WD primary ($M_a \approx 1.3 M_{\odot}$). Afterwards, the latter becomes a NS and after another 20 Myr a QS.

As a result of the mass loss, the secondary becomes a WD. The separation is very small ($\sim 0.3 R_\odot$) due to two earlier CE phases, so the secondary is able to fill its RL again due to gravitational radiation (GR). A long and stable MT phase proceeds during which the mass of the donor drops below $0.2 M_\odot$ (Fig. 4, middle plot).

The mass distributions of compact objects in LMXBs (Fig. 3) differ from those including all binary systems (Fig. 2). In models involving formation of QSs, we obtained a higher number of systems (22–67%) in the coexistence range. In general, the increase is more significant for higher values of M_{max}^H . In spite of this excess, the main peak of the mass distribution is still at $\sim 1.3 M_\odot$ (so outside of the coexistence range) and its position and magnitude are unaffected by the deconfinement. Indeed, most of the mass measurements are outside of the coexistence range, thus we cannot investigate the presence of this difference.

3.3. Double QSs

The main hindrance to the formation of double compact objects is the natal kick that may disrupt the binary during either of SN explosions. Nevertheless, we found an evolutionary route leading to the formation of double QS (DQS). Noteworthy, such scenario may be realized only in stellar populations with moderate metallicity ($Z = Z_\odot/10$). Only in such an environment we will observe a higher number of DQS/double NS in the coexistence range in comparison to model without deconfinement (f_{cr} ; see Tab. 1). For Z_\odot , or $Z_\odot/100$ metallicity, the f_{cr} fraction is < 1 , which marks the fact that the deconfinement in general hinders the formation of double compact objects by ~ 0.1 –3.0%.

\mathcal{R}_{DQS} ; *Double QS binary*— Typically, a DQS originates from a binary which on ZAMS consists of two stars with masses ~ 20 – $24 M_\odot$, where the primary is on the average only slightly ($\sim 1 M_\odot$) heavier than the secondary. The orbit must be wide enough to accommodate these stars (570 – $1000 R_\odot$). In a typical system, at the age of ~ 9 Myr, the primary fills the RL during the core helium burning phase and transfers mass onto the secondary. After the MT phase, the primary becomes an $\sim 8.2 M_\odot$ helium star with $\sim 29 M_\odot$ core helium burning companion. After 200 kyr, the secondary expands, fills the RL and commences the CE phase. The separation shrinks to a few R_\odot and the double helium star forms. The primary and the secondary sequentially (after 300 and 500 kyr, correspondingly) explode and form two QSs directly (like in $\mathcal{R}_{\text{A,dir}}$ scenario). The system has a high chance of surviving and forming a DQS on an orbit of 7.5 – $24 R_\odot$ (Fig. 4, lower plot).

The presented scenario does not work for solar metallicity (Z_\odot). The reason for that is a strong expansion of high- Z stars. The RL is filled earlier for the same initial separation (when the primary is on the HG), then for $Z = Z_\odot/10$ (primary is on a core helium burning). Consequently, the mass-loss is faster and longer, so the helium star forms earlier. This results in the SN explosion happening before the CE phase may commence and this shortens significantly the separation. Therefore, the orbit is larger ($\sim 1000 R_\odot$) in comparison to post CE systems ($\sim 10 R_\odot$), what leads to a system disruption during SNe.

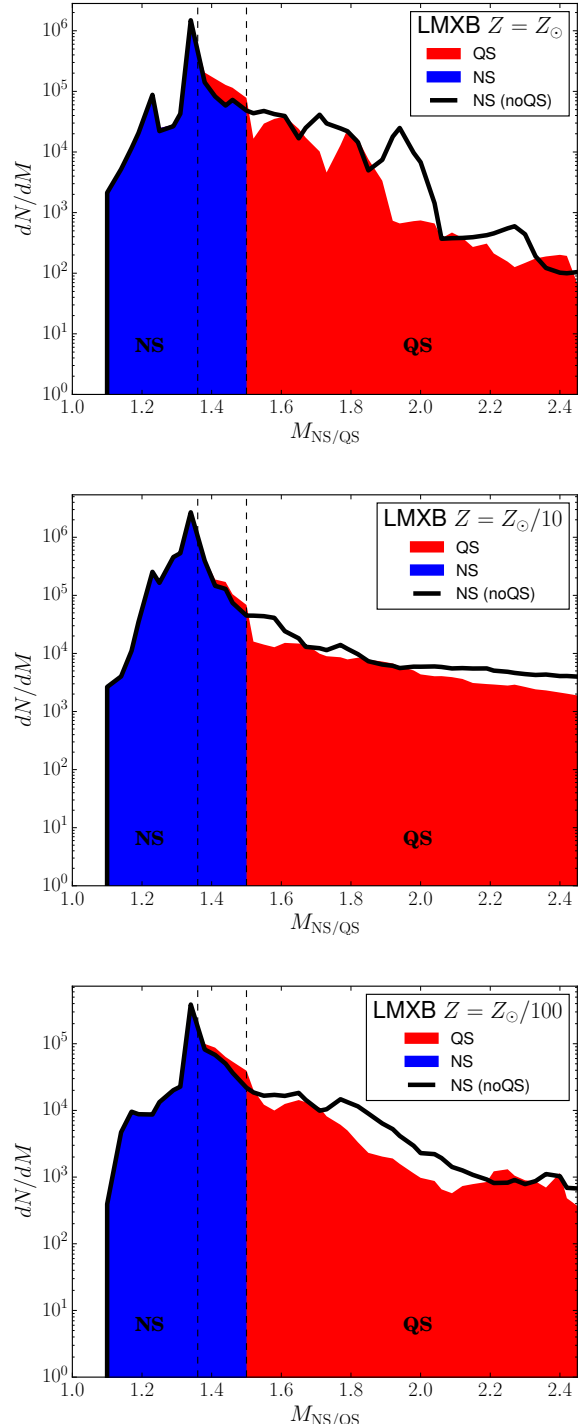


FIG. 3.— The distribution of masses for NS (blue) and QS (red) in LMXBs for metallicity $Z = Z_\odot$ (upper plot), $Z = Z_\odot/10$ (middle plot), and $Z = Z_\odot/100$ (lower plot). The LMXB is defined as a mass-transferring binary with NS/QS accretor. The black line marks the distribution of NSs’ masses in model without QSs (noQS). Features seen in the QS mass distribution are related to post-QS-formation evolution and are not a subject of this study.

There are no DQS in the lowest- Z environments ($Z_\odot/100$) neither, but for a different reason. Low-metallicity stars have small wind mass-loss rate. Additionally, their expansion rate is smaller than for higher- Z stars. This results in a lower chance of MT occurrence

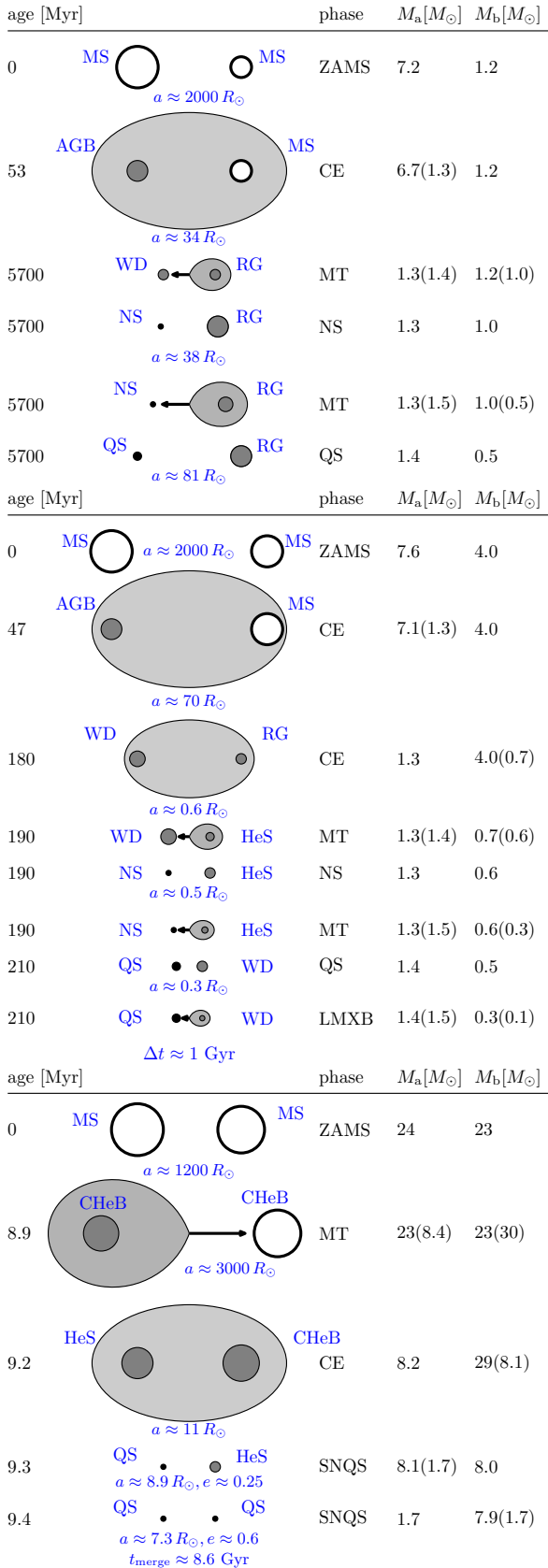


FIG. 4.— Schematic representation of a typical binary evolution leading to the formation of a QS (upper plot), LMXB with a QS (middle plot), or a double QS (lower plot). a is a separation and e is an eccentricity. Abbreviation are explained in Tab. 2. For details see Sec. 3.1.

during the core helium burning phase. As a consequence, after the MT phase, the primary is still massive and forms a BH. For lower-mass primaries the problem is still present as the expansion is small and it is hard to commence a CE phase and to shrink the orbit before the second SN. As a result, the system becomes disrupted when the second SN occurs.

The estimated merger rate of DQSs due to GR (Peters 1964) is ~ 71 events $\text{Gyr}^{-1} M_{\text{MWEG}}^{-1}$. An average time to coalescence after the formation of the second QS is about 10,000 Gyr and only a few systems are compact enough to merge within the Hubble time. In the case of the MW galaxy, low- Z stars are present mainly in the bulge, which constitutes only $\sim 1/6$ of the Galactic mass (Licquia & Newman 2015). Therefore, we estimate the merger rate for the MW as ~ 12 events Gyr^{-1} assuming a constant star formation rate.

3.4. Importance of the value of the limiting gravitational mass of NSs (M_{max}^H)

We found that our results change only quantitatively with different values of M_{max}^H . The formation of QSs occurs through the same evolutionary routes and the differences in the coexistence range, which for $M_{\text{max}}^H = 1.6 M_\odot$ is between $1.46 - 1.6 M_\odot$, are also small (30–72%). Tab. 4 provides results for the two values of $M_{\text{max}}^H = 1.5$ or $1.6 M_\odot$. The #QS changes by a factor of ~ 2 . The $\mathcal{R}_{\text{A,acc}}$ is the main evolutionary route for both models with more than 72% of QSs forming through this scenario. The fraction of LMXBs is similar for both values of M_{max}^H (difference of $\lesssim 4\%$).

A significant difference was obtained for the number of DQS, which dropped by nearly two orders of magnitude. The higher value of M_{max}^H requires higher initial stellar masses, as both QSs form directly after the SN (not as a result of mass accretion). Massive stars are less numerous on ZAMS, therefore DQSs have less progenitors for higher M_{max}^H .

4. DISCUSSION

4.1. A comparison with a previous study

Belczynski et al. (2002a) performed a population synthesis study of a QS population with the use of the earlier version of the *StarTrack* code. They found that QSs may constitute $\sim 10\%$ of all compact objects and noted that most of them in the Galaxy will be single rather than bound with companions. The current version of the *StarTrack* code has been significantly updated since that paper (see Sec. 2). Moreover, we incorporated a much more realistic model of QSs based on the two-families scenario. Belczynski et al. (2002a) just assumed that a fraction of stars in a particular mass range represent QSs.

Nevertheless, our results mostly agree with those of Belczynski et al. (2002a). We also found that the majority of QSs in the MW galaxy exist as single stars and that their number, although being significantly smaller than the number of NSs, is comparable with the number of BHs. The present study is also broader as it involves additionally an analysis of the formation scenarios, DQS mergers, and LMXBs.

4.2. Comparison with observations

TABLE 4
COMPARISON OF MODELS WITH $M_{\max}^H = 1.5 M_{\odot}$ AND $1.6 M_{\odot}$

$M_{\max}^H [M_{\odot}]$	$Z = Z_{\odot}$		$Z = Z_{\odot}/10$		$Z = Z_{\odot}/100$	
	1.5	1.6	1.5	1.6	1.5	1.6
#QS	9.0×10^4 (1%)	4.6×10^4 (1%)	2.7×10^5 (4%)	1.3×10^5 (2%)	1.5×10^5 (1%)	2.0×10^5 (2%)
$\mathcal{R}_{A,acc}$	8.6×10^4 (96%)	4.3×10^4 (94%)	2.1×10^5 (79%)	9.1×10^4 (72%)	1.2×10^5 (80%)	1.8×10^5 (93%)
$\mathcal{R}_{A,dir}$	4.0×10^3 (4%)	1.1×10^3 (2%)	2.6×10^4 (10%)	8.8×10^3 (8%)	3.2×10^3 (2%)	9.5×10^2 (1%)
$\mathcal{R}_{B,dir}$	6.5×10^2 ($\lesssim 1\%$)	1.8×10^4 (4%)	2.8×10^4 (11%)	2.5×10^4 (20%)	2.7×10^4 (18%)	1.3×10^4 (6%)
\mathcal{R}_{LMXB}	1.6×10^4 (18%)	6.5×10^3 (14%)	1.2×10^4 (4%)	6.0×10^3 (5%)	7.0×10^3 (5%)	5.8×10^3 (3%)
\mathcal{R}_{DQS}	–	–	4.2×10^3 (8%)	3.5×10^3 (1%)	–	–

NOTE. — The table shows present numbers of QSs per MWEG for models with different limiting mass (M_{\max}^H) and different metallicities. Results are shown both for the entire population and specific evolutionary routes. Numbers in parenthesis represent: for #QS: fraction of all compact objects (NS or QS; f_{QS}); evolutionary routes: fraction of #QS; \mathcal{R}_{DQS} : fraction of all double compact objects (NS or QS). See Sec. 3.4 for discussion.

The deconfinement process modifies the mass distribution of compact stars in the coexistence range. (Figs. 2 and 3). Our calculations predict 10–57% more binaries in models involving deconfinement than in models without it (noQS). For LMXBs this excess is even more pronounced (22–61%). For $M_{\max}^H = 1.6$ the excess is larger: 57–72% for all binaries, and 30–67% for LMXBs, but corresponds to a less populated range of masses and, therefore, will be even harder to detect. Nevertheless, the peak of the compact object mass distribution is located outside of the coexistence range, thus this range is a less populated part of the distribution. Consequently, current statistics of NS mass measurements (e.g. Ritter & Kolb 2003; Lattimer 2012; Özel & Freire 2016) are too small to prove or reject the presence of this excess. However, even just by having reliable mass distributions for compact objects, for example, in LMXBs or for millisecond radio pulsars (Kiziltan et al. 2013), one can try to study if some features are related to the presence of QSs in the population.

According to our results, most of the QSs are accompanied by WDs (78–95%). On average it is also true for LMXBs, but it is more model-dependent (7–84%). In general, the fraction of WDs is greater for higher metallicities, but seems to be independent on M_{\max}^H . Even if a QS formed with a RG companion ($\mathcal{R}_{A,acc}$), the counterpart will mostly become a WD at some age. Therefore, QSs will spend typically most of their life with a WD companion. As far as observations are concerned, Lattimer (2012) provided a list of NS mass measurements in binaries and the most typical companions appeared to be WDs. What makes WD the most typical companion is the long duration of this evolutionary stage. Therefore, we have higher chance of observing the system in that time. Although WDs are significantly lighter than QSs during MT, the resulting orbit expansion is counteracted by WD expansion and GR, what allows for a prolonged MT. It is easier to fill the RL by a companion which expands significantly due to nuclear evolution (e.g. MS, RG), however, a WD, if it manages to fill its RL, will provide a much longer MT phase.

In the near future more accreting compact objects can be identified in an X-ray survey made by eROSITA (Predehl et al. 2010) on-board Spectrum-RG satellite (to be launched in 2018). Systems with WD donors are of special interest, as in such cases accretors are expected to be massive. Accordingly, our simulations predict that WDs should be the most typical donors to LMXBs with QSs.

After accretion is over a compact object can be observed as a millisecond radio pulsar. It is expected that the new radio telescope FAST (Nan et al. 2011) can provide more sources of this kind.

4.3. Phenomenology of QSs in LMXBs

As one can notice from Tab. 4, the fraction of LMXBs containing a QS is not negligible, ranging from a few percent for low metallicities to almost 20% for solar metallicity. We estimated the rate of formation of QSs in LMXBs to be 19.5 (12.7) / 23.9 (16.7) / 15.8 (11.6) events Myr^{-1} MWEG $^{-1}$ for Z_{\odot} / 10% of Z_{\odot} / 1% of Z_{\odot} , respectively (numbers in parenthesis refer to model with $M_{\max}^H = 1.6 M_{\odot}$). Assuming that Milky-Way (MW) galaxy consists of 1/6 Population II stars and 5/6 Population I, we get an estimated number of ~ 13 –20 events Myr^{-1} in MW connected with NS to QS transition.

There are at least two possible observational implications of this result: the emission of a powerful electromagnetic signal in correspondence with the formation of a QS and the spin distribution of the pulsars in LMXBs.

The formation of a QS in a LMXB is a strongly exothermic process (releasing order of 10^{53} erg) and it can take place in a millisecond radio pulsar. These two properties strongly suggest a connection between the formation of a QS in a LMXB and at least a sub-class of GRBs within the protomagnetar model Metzger et al. (2011). It is remarkable that such a GRB would not be connected with the death of a massive star and thus with a SN. It is tempting to associate this possibility with the famous case of GRB060614 (Fynbo et al. 2006; Della Valle et al. 2006; Gal-Yam et al. 2006).

Although it is difficult to derive a frequency from just a single event we can try to compare the observed "rate" of GRBs lacking a SN with the rate of GRBs associated with the formation of a QS in a LMXB (mainly route $\mathcal{R}_{A,acc}$).

- The rate of NS to QS transitions in LMXBs is of the order of ~ 13 –20 events Myr^{-1} .
- A significant fraction, order of few tens percent, of compact stars in LMXBs rotates very rapidly and could possibly generate a GRB (always through the protomagnetar mechanism). This translates into a rate of GRBs associated with \mathcal{R}_{LMXB} of the order of one every 10^6 years.

- The fraction of long GRBs lacking a SN in respect to the GRBs for which an association with a SN has been clearly established to be of the order of 10% (Hjorth & Bloom 2012).
- The rate of long GRBs has been estimated to be of the order of one every $10^5 - 10^6$ years per galaxy (Podsiadlowski et al. 2004), therefore the rate of long GRBs non associated with a SN could be of the order of one every $10^6 - 10^7$ years. One can notice that the rate estimated in our model is fairly close to the observed one.

One should note that within the protomagnetar model a very strong magnetic field is needed. If this magnetic field is present before the formation of the QS, it may hinder the mass accretion. The magnetic field could instead be generated during the combustion from hadrons to quarks, which lasts a few seconds (Drago & Pagliara 2015). During the combustion the moment of inertia increases significantly (Pili et al. 2016) and it leads to the development of a strong differential rotation which in turn could generate the needed high magnetic field (Bucciantini et al. 2017).

The second possible phenomenological implication concerns the spin distribution of fast rotating pulsars in LMXBs. The increase of the moment of inertia resulting from the conversion of a NS into a QS implies a significant spin-down of the pulsar. In Pili et al. (2016) a change of the moment of inertia was large, up to a factor of two, implying a reduction of the spin frequency again by a factor of two. It is tempting to connect this effect with the bimodal distribution of the spin frequency found recently by Patruno et al. (2017) where the slowest component would contain a significant fraction of QSs in our scheme.

4.4. Strangelets pollution

The rate of mergers of DQS is crucial in order to estimate the production of strangelets, i.e. of lumps of stable strange quark matter, significantly smaller than a star. There are two known mechanisms by which strangelets could be produced: they could be produced at the time of primordial baryogenesis (when the temperature did fall below about 150 MeV) or they could be produced by partial fragmentation of at least one of the QSs at the beginning of the merging process of a DQS system⁴. The first process is uncertain (it has been criticized e.g. in Alcock & Farhi (1985)), but the second is very relevant as a potential source of strangelets. The existence of a significant flux of strangelets could trigger deconfinement in all compact stars at the moment of their formation (Madsen 1988), implying that only QSs can exist and therefore invalidating the two-families scenario. In order to clarify this issue two crucial information have to be provided: the rate of DQS mergers not directly collapsing into a BH and the probability of forming fragments (strangelets) in the mass range indicated above. An estimate of the first number has been obtained in this simulation. First, the number of DQS mergers is about 12

⁴ A further possible mechanism for strangelets production would be connected with an explosive conversion of hadronic stars into QSs (Jaikumar et al. 2007) but we follow the scheme presented in Sec. 2 and supported by the papers there quoted in which detonation is never obtained.

Gyr⁻¹ in our Galaxy, as stated above. Second, the total mass of the binary system exceeds $3M_{\odot}$ in most of the cases. Due to that many of these DQS systems collapse directly to a BH, as indicated by the analysis of Bauswein et al. (2009). The exact fraction of events in which the BH is not promptly formed is linked to M_{\max}^Q , but in any case it cannot exceed 12 events Gyr⁻¹.

Assuming, as an upper limit, that each event releases a mass of about $10^{-2}M_{\odot}$ (similar to the mass ejected in double NS mergers; the real number could be smaller by three/four orders of magnitude) one obtains an average strange quark matter density ρ_s in the Galaxy of about $(10^{-35} - 10^{-36}) \text{ g cm}^{-3}$. The flux of strangelets per unit of solid angle $dj_s/d\Omega$ can be estimated as follows by assuming that they all have the same baryon number A :

$$\frac{dj_s}{d\Omega} = \frac{\rho_s v}{4\pi A m_p}, \quad (1)$$

where v is the average velocity of the strangelets and m_p is the proton mass. By assuming that low mass strangelets have a velocity comparable to the velocity of the galactic halo i.e. $v = 250 \text{ km s}^{-1}$ one gets: $dj_s/d\Omega \sim 10^{-5} \rho_{35}/A \text{ cm}^{-2} \text{ s}^{-1} \text{ sr}^{-1}$ where $\rho_{35} = \rho_s/(10^{-35} \text{ g/cm}^3)$.

Having estimated an upper limit to the flux of strangelets it is possible to compare this limit with limits coming from Earth and Lunar experiments and with limits coming from astrophysics. Concerning the first type of limits, summarized in Price et al. (1984); De Rújula & Glashow (1984); Perillo Isaac et al. (1998); Weber (2005); Han et al. (2009), they are almost completely respected by our estimate of the flux. Only taking our very conservative upper limit on ρ_s , a small overlap with the constraints from the Lunar Soil experiment is found.

A more stringent constraint has been obtained recently by the PAMELA experiment (Adriani et al. 2015). Our upper limit on the flux would violate the observational limits for $A \lesssim 10^3$. On the other hand, the more realistic estimate quoted above fully satisfies the PAMELA limits.

Concerning the limits coming from astrophysics, the most relevant analysis has been done by Madsen (1988). First, even using our highest value of ρ_s the probability of capture of strangelets by a cold NS is negligible. This implies that pulsars displaying glitches (such as the Vela and the Crab pulsars) had a marginal chance to transform into QSs (which could not be able to glitch). In this way one of main mechanisms for the conversion of all NSs into QSs is ruled out.

According to Madsen, another possibility to trigger the formation of a QS is based on the capture of strangelets by main sequence stars: the strangelets would accumulate close to the core of the star and they would transform a NS into a QS soon after the SN explosion. In order to be captured by a main sequence star (and not to pass through it) strangelets need to have a baryon number smaller than $\sim 10^{28}$. This mechanism has two weak points. First, it is easy to demonstrate by using dimensional arguments that the strangelets dynamically ejected at the moment of the merger have a baryon number larger than about 10^{38} (Madsen 2002). Strangelet fragmentation through collisions, while quite efficient, could not be able to reduce the baryon number of the strangelets initially produced by ten orders of magnitude

(Bucciantini et al. 2017). Second, the strangelet located in the core of the collapsing star could evaporate due to the high temperatures reached at the moment of the bounce. Similar arguments can be applied to the case of molten NSs.

In conclusion, the limits stemming from Earth and Lunar experiments can be rather easily satisfied directly by our estimate of the upper limit on the flux without making any assumption on the fragmentation mechanism of the strangelets. Astrophysical limits are more subtle: in particular they depend on the ability of the strangelets to fragment into small nuggets and to survive temperatures of the order of few MeV.

4.5. Single QS population

Results of presented simulations show that formation of a QS in a binary system usually results in a disruption. Only in $\sim 3-10\%$ of cases the stars remain bound. As a result, about $(2.3-2.4) \times 10^6$ single QSs (depending on the model) originating from disrupted binaries should be present currently in a MWEG. Potentially it is possible to form a QS through single-star evolution providing the ZAMS mass of a star is in the range $M_{\text{ZAMS}} \approx 17-22 M_{\odot}$. However, most often so massive star are found in binaries (e.g. binary fraction $> 90\%$ found by Sana et al. 2014).

We note that a QS may be a result of a merger of a DQS. The number of such events is very low, as we show in Sec. 3.3. We do not consider this possibility here. Also, a few single QSs can result from NS-NS coalescence. Double NS coalescences have a rate of about one in 10–20 kyr in a MWEG (Postnov & Yungelson 2014). If in a few percent of such collisions stable QSs are formed (Drago et al., in prep.), then we have about a few tens of thousands of isolated QSs formed via this channel in a galactic lifetime.

5. SUMMARY AND CONCLUSIONS

We performed a population synthesis study of strange quark stars (QS). The two families scenario predicts that a neutron star (NS) becomes a QS after reaching the mass limit M_{max}^H (Drago et al. 2016), which we adopted to be 1.5, or $1.6 M_{\odot}$ in our modeling. Our results turn out to be rather robust respect to the variation of M_{max}^H . Notice anyway that in our analysis we have not included the effect of rapid rotation on the structure of the star. This will constitute the next extension of the present work.

Our analysis of QS population may be summarized as

follows:

- We found that QS may constitute $\sim 1-4\%$ of all compact objects in binaries (moreover, in our scheme all compact objects with masses larger than $\sim 1.5-1.6 M_{\odot}$ are QSs). Typically, a QS forms as a result of mass-accretion from a red giant companion onto a NS, however, a direct formation (immediately after the supernova explosion) is also possible in $\lesssim 30\%$ of cases.
- A relatively larger number of QS is predicted in low-mass X-ray binaries (3–18%) and especially in the coexistence range (22–72%). The effect on the mass distribution of compact stars is, however, too small to be detected using current observations. If future missions will provide better mass and radius measurements, it will be possible to test our predictions.
- Double QSs may constitute up to 8% of double compact objects with components masses below $2.5 M_{\odot}$. In most of the cases the two QSs do not merge within a Hubble time. We estimated a merger rate of ~ 12 events Gyr^{-1} for the Galactic bulge. Such a low rate implies a rather small “strangelets pollution” and in turn rules out at least one of the possible mechanisms suggested in the literature to convert all NSs into QSs. Moreover, all limits stemming from Earth and Lunar experiments are rather easily satisfied.
- The rate of conversion of a NS into a QS due to mass accretion in low-mass X-ray binaries is rather large, order of one event every 10^6 years. This process is strongly exothermic (it releases about 10^{53} erg) and it can take place in a rapid rotating compact star. These two properties suggest a possible connection with a special subclass of gamma-ray-bursts, possibly including GRB060614.

We want to thank thousands of volunteers who supported the research by participation in Universe@Home project⁵ and the anonymous referee for valuable comments. GW was partially supported by Polish NCN grant No. UMO-2015/19/B/ST9/03188. PS acknowledges support from the Russian Science Foundation grant 14-12-00146.

REFERENCES

- Abt, H. A. 1983, *ARA&A*, 21, 343
 Adriani, O., et al. 2015, *Phys. Rev. Lett.*, 115, 111101
 Alcock, C., & Farhi, E. 1985, *Phys. Rev.*, D32, 1273
 Alcock, C., Farhi, E., & Olinto, A. 1986, *ApJ*, 310, 261
 Alford, M. G., Burgio, G. F., Han, S., Taranto, G., & Zappalá, D. 2015, *Phys. Rev.*, D92, 083002
 Antoniadis, J., Freire, P. C. C., Wex, N., et al. 2013, *Science*, 340, 448
 Bauswein, A., Janka, H. T., Oechslin, R., et al. 2009, *Phys. Rev. Lett.*, 103, 011101
 Bejger, M., Zdunik, J. L., Haensel, P., & Fortin, M. 2011, *Astron. Astrophys.*, 536, A92
 Belczynski, K., Bulik, T., & Kluzniak, W. 2002a, *ApJ*, 567, L63
 Belczynski, K., Kalogera, V., & Bulik, T. 2002b, *ApJ*, 572, 407
 Belczynski, K., Kalogera, V., Rasio, F. A., et al. 2008, *ApJS*, 174, 223
 Bogdanov, S., Heinke, C. O., Özel, F., & Güver, T. 2016, *Astrophys. J.*, 831, 184
 Bombaci, I., & Datta, B. 2000, *Astrophys. J.*, 530, L69
 Bombaci, I., Parenti, I., & Vidana, I. 2004, *Astrophys. J.*, 614, 314
 Bucciantini, N., Drago, A., Pagliara, G., & Pili, A. 2017, in preparation
 Carilli, C. L., & Rawlings, S. 2004, *New Astron. Rev.*, 48, 979
 Chatterjee, D., & Vidaña, I. 2016, *European Physical Journal A*, 52, 29

⁵ <http://universeathome.pl>

- Cheng, K. S., & Dai, Z. G. 1996, *Physical Review Letters*, 77, 1210
- Dai, Z. G., & Lu, T. 1998, *Physical Review Letters*, 81, 4301
- De Rujula, A., & Glashow, S. L. 1984, *Nature*, 312, 734
- Della Valle, M., et al. 2006, *Nature*, 444, 1050
- Demorest, P. B., Pennucci, T., Ransom, S. M., Roberts, M. S. E., & Hessels, J. W. T. 2010, *Nature*, 467, 1081
- Drago, A., Lavagno, A., & Pagliara, G. 2014a, *Phys. Rev.*, D89, 043014
- Drago, A., Lavagno, A., Pagliara, G., & Pigato, D. 2014b, *Phys. Rev.*, C90, 065809
- Drago, A., Lavagno, A., Pagliara, G., & Pigato, D. 2016, *European Physical Journal A*, 52, 40
- Drago, A., Lavagno, A., & Parenti, I. 2007, *Astrophys. J.*, 659, 1519
- Drago, A., & Pagliara, G. 2015, *Phys. Rev.*, C92, 045801
- 2016, *Eur. Phys. J.*, A52, 41
- Drago, A., Pagliara, G., Pagliaroli, G., Villante, F. L., & Vissani, F. 2008, *AIP Conf. Proc.*, 1056, 256
- Duquenooy, A., & Mayor, M. 1991, *A&A*, 248, 485
- Furusawa, S., Sanada, T., & Yamada, S. 2016, *Phys. Rev.*, D93, 043019
- Fynbo, J. P. U., et al. 2006, *Nature*, 444, 1047
- Gal-Yam, A., et al. 2006, *Nature*, 444, 1053
- Gendreau, K. C., Arzoumanian, Z., & Okajima, T. 2012, in *Proc. SPIE, Vol. 8443, Space Telescopes and Instrumentation 2012: Ultraviolet to Gamma Ray*, 844313
- Guillot, S., & Rutledge, R. E. 2014, *Astrophys. J.*, 796, L3
- Haensel, P., Zdunik, J. L., & Schaeffer, R. 1986, *Astron. Astrophys.*, 160, 121
- Han, K., Ashenfelter, J., Chikarian, A., et al. 2009, *Phys. Rev. Lett.*, 103, 092302
- Herzog, M., & Röpke, F. K. 2011, *Phys. Rev.*, D84, 083002
- Hjorth, J., & Bloom, J. S. 2012, *CAPS*, 51, 169
- Horvath, J. E., & Benvenuto, O. G. 1988, *Phys. Lett.*, B213, 516
- Iida, K., & Sato, K. 1998, *Phys. Rev.*, C58, 2538
- Jaikumar, P., Meyer, B. S., Otsuki, K., & Ouyed, R. 2007, *Astron. Astrophys.*, 471, 227
- Jiang, L., Li, X.-D., Dey, J., & Dey, M. 2015, *ApJ*, 807, 41
- Kiziltan, B., Kottas, A., De Yoreo, M., & Thorsett, S. E. 2013, *ApJ*, 778, 66
- Kroupa, P., Tout, C. A., & Gilmore, G. 1993, *MNRAS*, 262, 545
- Lasky, P. D., Haskell, B., Ravi, V., Howell, E. J., & Coward, D. M. 2014, *Phys. Rev.*, D89, 047302
- Lattimer, J. M. 2012, *Annual Review of Nuclear and Particle Science*, 62, 485
- Li, A., Zhang, B., Zhang, N. B., et al. 2016, *Phys. Rev.*, D94, 083010
- Licquia, T. C., & Newman, J. A. 2015, *ApJ*, 806, 96
- Lu, H.-J., Zhang, B., Lei, W.-H., Li, Y., & Lasky, P. D. 2015, *Astrophys. J.*, 805, 89
- Madsen, J. 1988, *Phys. Rev. Lett.*, 61, 2909
- 2002, *J. Phys.*, G28, 1737
- 2005, *Phys. Rev.*, D71, 014026
- Metzger, B. D., Giannios, D., Thompson, T. A., Bucciantini, N., & Quataert, E. 2011, *Mon. Not. Roy. Astron. Soc.*, 413, 2031
- Miller, M. C., & Lamb, F. K. 2016, *European Physical Journal A*, 52, 63
- Nan, R., Li, D., Jin, C., et al. 2011, *International Journal of Modern Physics D*, 20, 989
- Niebergal, B., Ouyed, R., & Jaikumar, P. 2010, *Phys. Rev.*, C82, 062801
- Olinto, A. V. 1987, *Phys. Lett.*, B192, 71
- Ouyed, A., Ouyed, R., & Jaikumar, P. 2017, *arXiv:1706.05438*
- Özel, F., & Freire, P. 2016, *ARA&A*, 54, 401
- Özel, F., Psaltis, D., Güver, T., et al. 2016, *Astrophys. J.*, 820, 28
- Pagliara, G., Herzog, M., & Röpke, F. K. 2013, *Phys. Rev.*, D87, 103007
- Patruno, A., Haskell, B., & Andersson, N. 2017, *arXiv:1705.07669*
- Perillo Isaac, M. C., et al. 1998, *Phys. Rev. Lett.*, 81, 2416, [Erratum: *Phys. Rev. Lett.* 82, 2220 (1999)]
- Peters, P. C. 1964, *Physical Review*, 136, 1224
- Pili, A. G., Bucciantini, N., Drago, A., Pagliara, G., & Del Zanna, L. 2016, *Mon. Not. Roy. Astron. Soc.*, 462, L26
- Podsiadlowski, P., Mazzali, P. A., Nomoto, K., Lazzati, D., & Cappellaro, E. 2004, *Astrophys. J.*, 607, L17
- Popov, S. B., & Prokhorov, M. E. 2005, *A&A*, 434, 649
- 2007, *Physics Uspekhi*, 50, 1123
- Postnov, K. A., & Yungelson, L. R. 2014, *Living Reviews in Relativity*, 17, 3
- Predehl, P., Andritschke, R., Böhringer, H., et al. 2010, in *Proc. SPIE, Vol. 7732, Space Telescopes and Instrumentation 2010: Ultraviolet to Gamma Ray*, 77320U
- Price, P. B., Guo, S.-l., Ahlen, S. P., & Fleischer, R. L. 1984, *Phys. Rev. Lett.*, 52, 1265
- Ritter, H., & Kolb, U. 2003, *A&A*, 404, 301
- Sana, H., Le Bouquin, J.-B., Lacour, S., et al. 2014, *ApJS*, 215, 15
- Villante, F. L., Serenelli, A. M., Delahaye, F., & Pinsonneault, M. H. 2014, *ApJ*, 787, 13
- Weber, F. 2005, *Prog. Part. Nucl. Phys.*, 54, 193
- Wiktorowicz, G., Sobolewska, M., Sądowski, A., & Belczynski, K. 2015, *ApJ*, 810, 20
- Zhu, C., Lü, G., Wang, Z., & Liu, J. 2013, *PASP*, 125, 25